M. Doser, S. Aghion, C. Amsler, G. Bonomi, R.S. Brusa, M. Caccia, R. Caravita, F. Castelli, G. Cerchiari, D. Comparat, G. Consolati, A. Demetrio, L. Di Noto, C. Evans, M. Fanì, R. Ferragut, J. Fesel, A. Fontana, S. Gerber, M. Giammarchi, A. Gligorova, F. Guatieri, S. Haider, A. Hinterberger, H. Holmestad, A. Kellerbauer, O. Khalidova, D. Krasnický, V. Lagomarsino, P. Lansonneur, P. Lebrun, C. Malbrunot, S. Mariazzi, J. Marton, V. Matveev, Z. Mazzotta, S.R. Müller, G. Nebbia, P. Nedelec, M. Oberthaler, N. Pacifico, D. Pagano, L. Penasa, V. Petracek, F. Prelz, M. Prevedelli, B. Rienaecker, J. Robert, O.M. Røhne, A. Rotondi, H. Sandaker, R. Santoro, L. Smestad, F. Sorrentino, G. Testera, I.C. Tietje, E. Widmann, P. Yzombard, C. Zimmer, J. Zmeskal, N. Zurlo

AEgIS at ELENA: Outlook for Physics with a Pulsed Cold Antihydrogen Beam

Philosophical Transactions of the Royal Society A: Mathematical, Physical and Engineering Sciences, Vol. 376, N. 2116, 2018, 20170274 (10 pages)
doi:10.1098/rsta.2017.0274

PHILOSOPHICAL TRANSACTIONS A

rsta.royalsocietypublishing.org

Research

Cite this article: Doser M *et al*. 2018 AEgIS at ELENA: outlook for physics with a pulsed cold antihydrogen beam. *Phil. Trans. R. Soc. A* **376**: 20170274.
http://dx.doi.org/10.1098/rsta.2017.0274

Accepted: 5 December 2017

One contribution of 11 to a Theo Murphy meeting issue 'Antiproton physics in the ELENA era'.

Subject Areas:
atomic and molecular physics, particle physics

Keywords:
antihydrogen, antiprotons, positrons, positronium

Author for correspondence:
M. Doser
e-mail: michael.doser@cern.ch

AEgIS at ELENA: outlook for physics with a pulsed cold antihydrogen beam

M. Doser[1], S. Aghion[2,3], C. Amsler[4], G. Bonomi[5,6], R. S. Brusa[7,8], M. Caccia[3,9], R. Caravita[10,11], F. Castelli[3,12], G. Cerchiari[13], D. Comparat[14], G. Consolati[2,3], A. Demetrio[15], L. Di Noto[10,11], C. Evans[2,3], M. Fani'[1,10,11], R. Ferragut[2,3], J. Fesel[1], A. Fontana[6], S. Gerber[1], M. Giammarchi[3], A. Gligorova[4], F. Guatieri[7,8], S. Haider[1], A. Hinterberger[1], H. Holmestad[16], A. Kellerbauer[13], O. Khalidova[1], D. Krasnický[11], V. Lagomarsino[10,11], P. Lansonneur[17], P. Lebrun[17], C. Malbrunot[1,4], S. Mariazzi[18], J. Marton[4], V. Matveev[19,20], Z. Mazzotta[3,12], S. R. Müller[15], G. Nebbia[18], P. Nedelec[17], M. Oberthaler[15], N. Pacifico[1], D. Pagano[5,6], L. Penasa[7,8], V. Petracek[21], F. Prelz[3], M. Prevedelli[22], B. Rienaecker[1], J. Robert[14], O. M. Røhne[16], A. Rotondi[6,23], H. Sandaker[16], R. Santoro[3,9], L. Smestad[1,24], F. Sorrentino[11], G. Testera[11], I. C. Tietje[1], E. Widmann[4], P. Yzombard[13], C. Zimmer[1,13,25], J. Zmeskal[4] and N. Zurlo[6,26]

[1]Physics Department, CERN, 1211 Geneva 23, Switzerland
[2]Politecnico of Milano, Piazza Leonardo da Vinci 32, 20133 Milano, Italy
[3]INFN Milano, via Celoria 16, 20133 Milano, Italy
[4]Stefan Meyer Institute for Subatomic Physics, Austrian Academy of Sciences, Boltzmanngasse 3, 1090 Vienna, Austria

THE ROYAL SOCIETY PUBLISHING

[5]Department of Mechanical and Industrial Engineering, University of Brescia, via Branze 38, 25123 Brescia, Italy
[6]INFN Pavia, via Bassi 6, 27100 Pavia, Italy
[7]Department of Physics, University of Trento, via Sommarive 14, 38123 Povo, Trento, Italy
[8]TIFPA/INFN Trento, via Sommarive 14, 38123 Povo, Trento, Italy
[9]Department of Science, University of Insubria, via Valleggio 11, 22100 Como, Italy
[10]Department of Physics, University of Genova, via Dodecaneso 33, 16146 Genova, Italy
[11]INFN Genova, via Dodecaneso 33, 16146 Genova, Italy
[12]Department of Physics, University of Milano, via Celoria 16, 20133 Milano, Italy
[13]Max Planck Institute for Nuclear Physics, Saupfercheckweg 1, 69117 Heidelberg, Germany
[14]Laboratoire Aimé Cotton, Université Paris-Sud, ENS Cachan, CNRS, Université Paris-Saclay, 91405 Orsay Cedex, France
[15]Kirchhoff-Institute for Physics, Heidelberg University, Im Neuenheimer Feld 227, 69120 Heidelberg, Germany
[16]Department of Physics, University of Oslo, Sem Slandsvei 24, 0371 Oslo, Norway
[17]Institute of Nuclear Physics, CNRS/IN2p3, University of Lyon 1, 69622 Villeurbanne, France
[18]INFN Padova, via Marzolo 8, 35131 Padova, Italy
[19]Institute for Nuclear Research of the Russian Academy of Science, Moscow 117312, Russia
[20]Joint Institute for Nuclear Research, 141980 Dubna, Russia
[21]Czech Technical University in Prague, Brehová 7, 11519 Prague 1, Czech Republic
[22]University of Bologna, Viale Berti Pichat 6/2, 40126 Bologna, Italy
[23]Department of Physics, University of Pavia, via Bassi 6, 27100 Pavia, Italy
[24]The Research Council of Norway, PO Box 564, 1327 Lysaker, Norway
[25]Department of Physics, Heidelberg University, Im Neuenheimer Feld 226, 69120 Heidelberg, Germany
[26]Department of Civil Engineering, University of Brescia, via Branze 43, 25123 Brescia, Italy

MD, 0000-0002-3618-0889

The efficient production of cold antihydrogen atoms in particle traps at CERN's Antiproton Decelerator has opened up the possibility of performing direct measurements of the Earth's gravitational acceleration on purely antimatter bodies. The goal of the AEgIS collaboration is to measure the value of g for antimatter using a pulsed source of cold antihydrogen and a Moiré deflectometer/Talbot–Lau interferometer. The same antihydrogen beam is also very well suited to measuring precisely the ground-state hyperfine splitting of the anti-atom. The antihydrogen formation mechanism chosen by AEgIS is resonant charge exchange between cold antiprotons and Rydberg positronium. A series of technical developments regarding positrons and positronium (Ps formation in a dedicated room-temperature target, spectroscopy of the $n = 1$–3 and $n = 3$–15 transitions in Ps, Ps formation in a target at 10 K inside the 1 T magnetic field of the experiment) as well as antiprotons (high-efficiency trapping of $\bar{p}$, radial compression to sub-millimetre radii of mixed $e^-/\bar{p}$ plasmas in 1 T field, high-efficiency transfer of $\bar{p}$ to the antihydrogen production trap using an in-flight launch and recapture procedure) were successfully implemented. Two further critical steps that are germane mainly to charge exchange formation of antihydrogen—cooling of antiprotons and formation of a beam of antihydrogen—are being addressed in parallel. The coming of ELENA will allow, in the very near future, the number of trappable antiprotons to be increased by more than a factor of 50. For the antihydrogen production scheme chosen by AEgIS, this will be reflected in a corresponding

increase of produced antihydrogen atoms, leading to a significant reduction of measurement times and providing a path towards high-precision measurements.

This article is part of the Theo Murphy meeting issue 'Antiproton physics in the ELENA era'.

1. Introduction and overview

The primary scientific goal of AEgIS [1] is the direct measurement of the Earth's local gravitational acceleration g on antihydrogen ($\bar{H}$). The experiment is designed to carry out a gravity measurement with antimatter by observing the vertical displacement (using a high-resolution position-sensitive detector) of the shadow image produced by an $\bar{H}$ beam, formed by its passage through a Moiré deflectometer [2], the classical counterpart of a matter wave interferometer.

A second goal of the experiment is to carry out spectroscopic measurements on the antihydrogen atoms in flight; specifically, we intend to use the advantages (see §2) that a pulsed cold beam of antihydrogen offers to carry out a measurement of the ground-state hyperfine splitting (HFS) of antihydrogen.

The advent of ELENA and concomitant changes will have a significant impact on the physics reach of the AEgIS experiment, whose techniques should benefit significantly from the increased number of trappable antiprotons, and also from altered operating conditions, ranging from continuous beam availability to extensions of the experimental zone, allowing an expanded range of spectroscopy options with respect to the present situation.

2. Advantages of an antihydrogen beam

The AEgIs collaboration has focused on carrying out measurements on a beam of antihydrogen atoms for a number of reasons. Gravitational effects in particular are easily masked by couplings of the antimatter probes to other fields, particularly magnetic fields and their gradients. While shielding of magnetic fields close to the environment of a Penning trap to sub-μG levels has been established [3], a level allowing one in principle to also work with Rydberg antihydrogen, achieving a homogeneity of better than only 1 part in 10^4 inside a magnet is already very challenging. An additional advantage of extracting a beam of atoms into a region outside of magnets encased in cryostats is the greater geometrical access that this allows for laser light, for example, in contrast to the very strong constraints imposed by a radially limited Penning trap environment deeply embedded inside a magnet.

By separating the formation from the physics measurement region, a beam allows greater flexibility and control; for cold enough beams (velocity $\sim 1000\,\mathrm{m\,s^{-1}}$), the interaction time between the antihydrogen atoms and the external fields is long: interaction times of the order of milliseconds are sufficient to already measurably influence the studied system. For Talbot–Lau gravity measurements, as well as for HFS measurements, a continuous cold beam is already sufficient. Pulsed beam production affords an additional handle, as it not only defines the initial conditions of the atoms, but also sets a well-determined time window which can be used for atom manipulations, in addition to providing the possibility of velocity tagging each atom upon annihilation. An additional benefit is that the pulsed nature of the production process strongly reduces any potential background signals, as observables can be limited to specific time intervals.

3. Formation method

The production of a pulsed cold beam of $\bar{H}$, and thus both the measurement of g as well as a precise determination of the HFS of antihydrogen with AEgIS, build upon the initial concept [4–6] and experimental demonstration [7] of charge exchange production of antihydrogen, as well as on

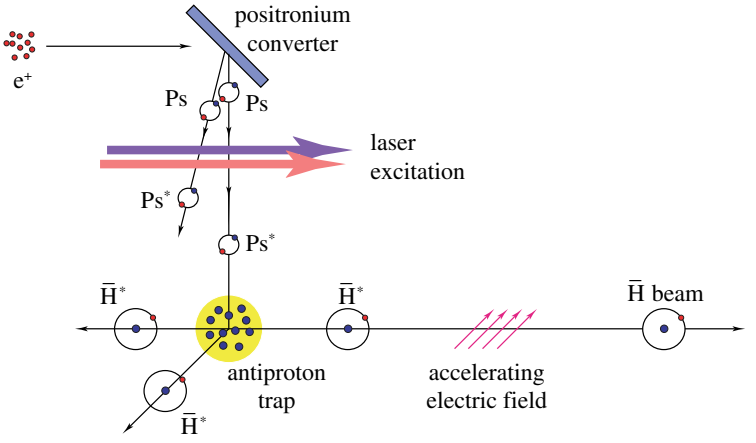

Figure 1. Foreseen method for the production of a pulsed beam of cold $\bar{H}$ atoms. Antiprotons are trapped and cooled inside a Penning–Malmberg trap. The separation between this trap (formed by a stack of cylindrical electrodes) and the positronium production target is approximately 15 mm. Positrons are injected at several kilovolts parallel to the solenoidal magnetic field through a second parallel stack of electrodes into the target (positronium converter) to form positronium, which is laser-excited into a Rydberg state before interacting with antiprotons to form Rydberg antihydrogen atoms. These will be accelerated by an electric field gradient parallel to the magnetic field to form a beam. (Online version in colour.)

the technique of Stark acceleration (for a recent review of Stark deceleration of Rydberg systems, see [8]). Specifically, the experimental steps are the following (figure 1):

— production of positrons (e^+) via a ^{22}Na source and accumulator;
— capture and accumulation of $\bar{p}$ from the Antiproton Decelerator (AD) in a Penning–Malmberg trap in a 4.46 T magnetic field;
— cooling of the $\bar{p}$ to cryogenic temperatures in a 1 T magnetic field;
— production of positronium (Ps) by implantation of an intense e^+ pulse into a cryogenic nanoporous target in the vicinity of the antiprotons;
— excitation of the Ps to a Rydberg state with principal quantum number $n \sim 15$;
— pulsed formation of $\bar{H}$ by resonant charge exchange between Rydberg Ps and cold $\bar{p}$; and
— pulsed formation of an $\bar{H}$ beam by Stark acceleration with inhomogeneous electric fields.

4. Positronium formation and laser excitation

In a first important step towards establishing its pulsed antihydrogen beam formation scheme, AEgIS has implemented the techniques needed to form and laser-excite positronium into a Rydberg state (first demonstrated by [9] for a different pathway than the one chosen in AEgIS) in a (magnetic-field-free) test chamber outside of the main apparatus [10], a crucial part of the charge exchange reaction between positronium (Ps) excited into a Rydberg state and an antiproton. The pathway chosen by AEgIS for this excitation process proceeds via a two-step laser excitation, from ground state to $n = 3$ ($\lambda = 205$ nm), and then to the Rydberg band ($\lambda \sim 1710$ nm). Figure 2 shows the annihilation lifetime spectra of Ps manipulated with different laser frequencies.

To form positronium in the proximity of the antiprotons held in a Malmberg–Penning trap inside a 1 T magnet, positrons are extracted from the accumulator and launched via a transfer section towards the target following off-axis trajectories without being re-caught in the 5 T or 1 T traps. The formation of low-energy Ps requires implanting e^+ in the target material deeply enough that the formed Ps have time to cool by collisions with the target channel walls. Typically, this is achieved by sending e^+ towards the target with a few keV energy.

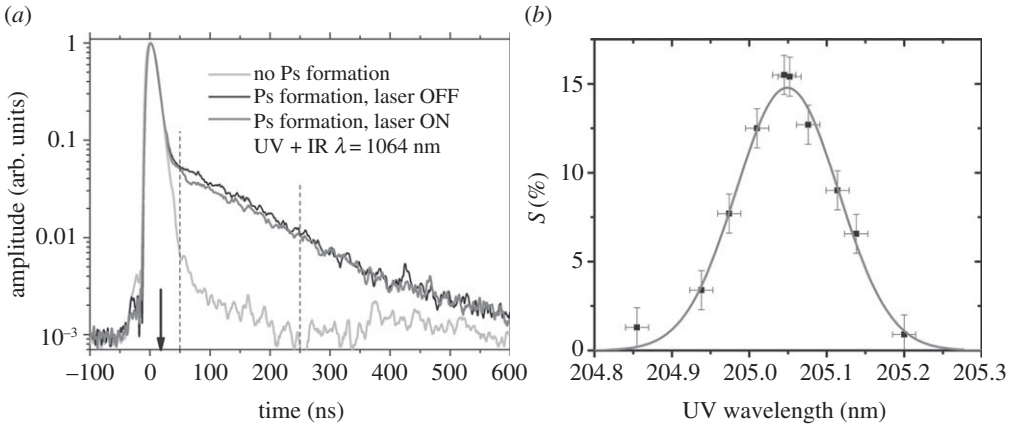

Figure 2. (*a*) Single-shot positronium annihilation lifetime (SSPALS [11]) spectra of background in light grey line, Ps into vacuum with laser OFF in black and UV + IR lasers ON (205.05 + 1064 nm) in dark grey. Each spectrum is the average of 15 single shots. The arrow marks the time when the laser is shot onto the Ps cloud (16 ns after the prompt peak). The difference in the area between 50 and 250 ns after the prompt peak (vertical dashed lines) for laser ON and laser OFF is used to evaluate the fraction of quenched or ionized o-Ps atoms *S* (%) for $n = 3$ [10]. (*b*) Resonance curve of the $1\,^3S{-}3\,^3P$ Ps excitation obtained by scanning the UV laser wavelength for constant IR wavelength. Each point has been calculated by averaging 15 SSPALS spectra. Statistical errors (on the *y*-axis) and accuracy (on the *x*-axis) are discussed in [10], along with a description of the fitting function used.

The energy of the e^+ extracted from the accumulator is limited to 300 eV and thus the acceleration must be achieved during their passage through the transfer section. The acceleration stage is in the form of a simple kicker: a single cylindrical electrode mounted along the transfer line, initially grounded and quickly (with a risetime of a few nanoseconds) pulsed to $V_{\mathrm{kick}} \sim 5$ kV when all the e^+ are inside it. All positrons gain an energy eV_{kick} when they exit the tube. Direct positron transport to the target sited inside the 1 T magnet, injection into the target at 5 keV, as well as formation of positronium, have been established. The final step is laser excitation of the formed positronium using the same lasers as previously used to carry out the two-step formation of Rydberg positronium in the external positronium test set-up.

5. Antiproton plasma manipulations

Antiprotons from the AD are efficiently (approx. 1% of incoming antiprotons) trapped in a 4.46 T magnetic field. The formation region of antihydrogen atoms must be sited in a low (1 T) magnetic field (in order to avoid field ionization of the formed Ps* and to facilitate Stark acceleration of formed $\bar{\mathrm{H}}^*$). It must also be in close proximity to the positronium formation target to maximize the solid angle for useful Rydberg Ps. Consequently, the particle trap electrode radius of this 'production' trap is only 5 mm and the trap electrodes themselves are partly constituted of a mesh to allow the passage of Ps* produced 15 mm away. Minimizing the radial dimensions of the antiproton plasma prior to transfer from the catching trap to the production trap is thus of paramount importance, all the more so as the change in magnetic field between the 5 T and the 1 T regions leads to a substantial increase in the radial size of the plasma during transfer.

Antiprotons are transferred ballistically from the 5 T catching and cooling trap to the 1 T antihydrogen production trap, where they are re-caught in flight, with an efficiency of more than 80% (the transfer procedure itself has higher efficiency, but some losses due to the heating inherent in the transfer procedure occur subsequent to the transfer) and low expansion in a multi-step procedure. This ballistic transfer combines the advantages of the efficient antiproton compression

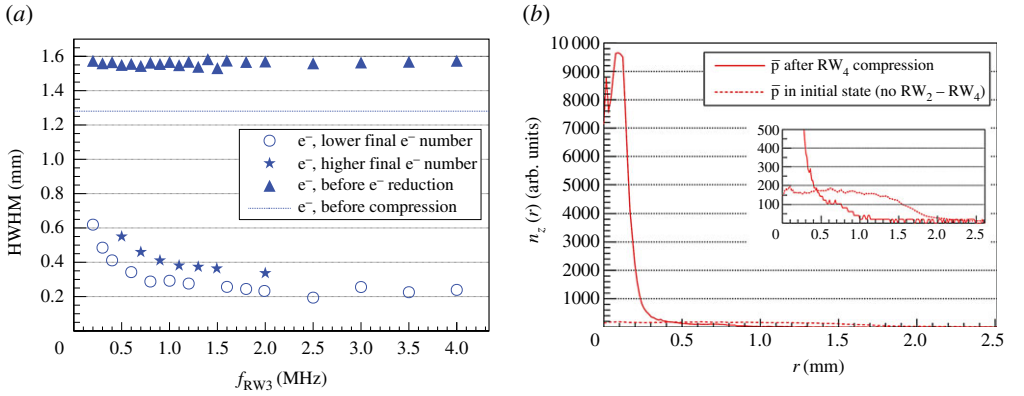

Figure 3. (*a*) HWHM of electrons versus the frequency of the second step rotating wall during the two-step $\bar{p}$ RW compression procedure. When more electrons remain in the trap after the partial e^- removal (star-marked points), compression is less pronounced. The dotted lines indicate the particle cloud radius after the e^- reduction before turning on the RW drive. (*b*) Antiproton radial profile before (dotted line) and after (solid line) multi-step RW compression with (third step) $f_{RW4} = 2$ MHz and $A_{RW4} = 0.5$ V. The inset shows the same figure zoomed to see the original $\bar{p}$ distribution before compression. During this procedure, two e^- reduction steps were applied and, in total, three $\bar{p}$ RW compression steps were used. The $\bar{p}$ plasma HWHM was 1.63 mm before and 0.17 mm after the compression. (Online version in colour.)

in the 5 T region (see below) with a transfer procedure that does not induce any additional radial expansion (beyond that caused by the change in magnetic field), as would be the case for a slower adiabatic transfer.

Compression of the antiproton cloud (more exactly, of the mixed $\bar{p}$ and e^- plasma) is itself a multi-step process, which alternates rotating wall (RW) steps with electron removal steps [12]. We have performed compression of a mixed $\bar{p}$ and e^- plasma trapped in a cryogenic Penning–Malmberg trap and achieved high antiproton densities ($n_{\bar{p}} \sim 10^{13}\,m^{-3}$). The compression procedure was accompanied with partial electron number reduction to achieve the lowest $\bar{p}$ radius of $r_{\bar{p}} = 0.17$ mm (figure 3*b*); this radius can be tuned by an appropriate choice of the frequency applied (figure 3*a*).

In order to achieve such strong compression, in which the antiproton distribution follows that of the electrons, it is crucial to compress with high efficiency the electron cloud, including possible electron tail structures that might remain at larger radii. Such electron tails may have been overlooked in past work on the RW drive compression of antiprotons and electrons (e.g. [13]), and turn out to be crucial in achieving antiproton cloud radii as low as 0.17 mm in a 4.46 T trap.

6. Improvements: rate, temperature

While the expected baseline antihydrogen production parameters should be enough to perform a wide range of physics measurements (gravity, spectroscopy), particularly in combination with the expected increase of antiprotons that becomes available with ELENA, several reasons encourage exploring techniques that would further increase the number and decrease the temperature of formed antihydrogen atoms, which in turn should allow longer, and thus more precise, measurements.

On the one hand, a number of measurements are expected to be statistically limited, in particular measurements on gravitationally deflected antihydrogen beams (as the effect of external field gradients, one of the main systematics, can be kept to levels that do not play a role at the per cent level [3]). On the other hand, only few antiproton cooling techniques exist that would lead to forming antihydrogen with temperatures of O(K) through charge exchange (for

which the antiproton temperature plays the dominant role); one of these is evaporative cooling of antiprotons [14]. This technique, however, is accompanied by the loss of large numbers of antiprotons, and thus reduces the number of potentially formable cold antihydrogen atoms.

Starting from lower-temperature antiprotons before applying evaporative cooling, or even better, reaching low enough temperatures that the recoil from impinging positronium begins to significantly contribute to the momentum of the produced antihydrogen atom, is thus a goal worth pursuing. Work on laser cooling of anions (to sympathetically cool antiprotons) and on improved Ps production is thus a high priority of the collaboration.

When positronium is produced in a production target, the critical numbers for the formation of antihydrogen are the relative velocity between antiprotons and positronium [5,15], the number of antiprotons that (Rydberg) positronium sees, and the number of (Rydberg) positronium atoms emitted into the solid angle subtended by the antiproton cloud. Influencing the first component would require slowing positronium to approximately $10^4\,\mathrm{m\,s^{-1}}$ (or less), while the second term is defined by the trapping efficiency of antiprotons, which is currently at approximately 1%, and should increase to around 50% with ELENA for an appropriate choice of degrader. The third term is defined by the degree to which emission of positronium from the production target is isotropic, as well as by the distance between this target and the trapped antiprotons.

In the AEgIS design, this third element can be improved: the baseline design places the positronium production target at a distance of 15 mm from the antiprotons (figure 1), preventing more than 99% of the positronium from interacting with the antiprotons. Reducing this distance by further decreasing the radius of the Penning trap holding the antiprotons as well as those guiding the positrons is highly challenging. Instead, it might be possible to produce positronium in approximately 1 μm transmission foils [16], which could be placed at a few millimetres from the antiprotons, inside the Penning trap electrodes. Obviously, placing such (insulating) membranes within the Penning trap environment would affect the homogeneity of its electrical potential, which would require encasing it in shielding grids. In preparation for tests of shielding with electrons, we have started work on producing thin membranes that would be suitable for transmission positronium production. The first such technology to be tested [17,18] consists of columnar silicon towers grown on top of 20 nm carbon foils. The resulting yield of o-Ps of 10% still lies below that of reflection targets, which have a yield of 30% or more. Nevertheless, these first results are promising, and work is ongoing on growing thicker membranes, as well as producing other types of membranes.

The second area of active research concerns the possibility of sympathetically cooling antiprotons via laser-cooled anions [19,20]. The velocity of antihydrogen atoms produced via charge exchange is dominated by that of the antiprotons prior to charge exchange, at least for antiprotons with temperatures above approximately 50 mK. Sympathetic cooling with laser-cooled anions in principle allows reaching such low temperatures [21]. Two paths being pursued—laser cooling of La^- [22,23] and laser cooling of C_2^- [24]—promise to converge in the near future, bringing ultra-low-temperature antiprotons, and thus ultra-low-temperature antihydrogen, within reach.

Until now, only three atomic elements have been identified whose anions have a bound–bound electric-dipole transition potentially amenable to laser cooling. We have been focusing on the lanthanum anion, which had been predicted to exhibit a suitable transition based on theoretical calculations [20,22]. This transition, between the $5d^26s^2\ {}^3F_2^e$ ground state and the $5d6s^26p\ {}^3D_1^o$ excited state in La^-, in the mid-IR wavelength range, has been fully characterized by collinear laser spectroscopy [23]. As one of the main results, the resonant cross-section was found to be in the range of $10^{-12}\,\mathrm{cm^2}$, which means that the expected cooling rate of several kHz is the highest of the known anion laser cooling candidates. Figure 4*a* shows the full level scheme of the states relevant for laser cooling, including their HFS. A sketch of the Paul trap in which first cooling of La^- will be attempted is shown in figure 4*b*.

In parallel, work on the molecular anion C_2^- [24], whose energy levels are already very well known, and which has a smaller mass ratio to antiprotons than lanthanum, is under way. C_2^- exhibits a $B^2\Sigma(v'=0) \leftrightarrow X^2\Sigma(v''=0)$ system and a $A^2\Pi_{1/2}(v'=0) \leftrightarrow X^2\Sigma(v''=0)$ system with 72%

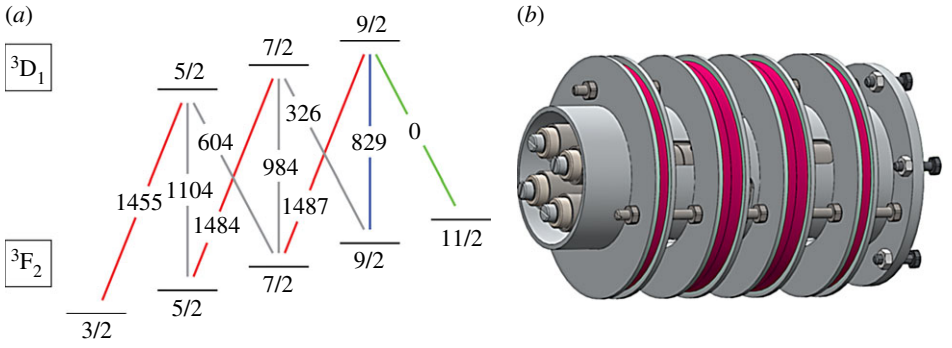

Figure 4. (*a*) Energy level diagram of the relevant states for laser cooling of La^-, including hyperfine splitting of the states due to the nuclear spin [23]. The (red, 1455, 1484 and 1487) coloured lines between the hyperfine sublevels indicate the three required laser wavelengths (the numbers next to the lines correspond to the detuning of the transition frequencies, in MHz, relative to the $F = \frac{11}{2} \rightarrow \frac{9}{2}$ transition, which lies at 96.592004(86) THz). (*b*) Sketch of the radiofrequency Paul trap which will be used to demonstrate the laser cooling of La^- in the absence of a magnetic field. The disc-shaped structures shown in magenta held by the clamping rings are permanent magnets which compensate for the residual magnetic field at the location of the Paul trap due to the Penning trap a short distance upstream. (Online version in colour.)

and 96% branching ratios, respectively. The lifetime of the A state is 50 μs with wavelengths of 2.53 μm (branching ratio of 96%) and 4.57 μm (branching ratio of 4%). In order to close the rotational transition cycle, two lasers are required for each of these vibrational transitions to couple $X(N'' = 0, 2)$ to $A(N' = 1, J' = \frac{1}{2})$. The C_2^- anion has the notable advantage of not presenting any hyperfine structure [25].

7. Outlook for ELENA

Charge exchange formation of antihydrogen should significantly benefit from the increased trappable flux of antiprotons that ELENA provides. For the present experimental parameters, an expected 50-fold increase in the number of trappable antiprotons should scale linearly in the number of antihydrogen atoms expected to be produced. Also for sub-K antiprotons, the velocity due to the plasma magnetron rotation does not begin to be a limitation until the density reaches approximately $10^{13}\,m^{-3}$, a peak value that can already be reached by AEgIS. To remain below this limit with increased numbers of antiprotons will require working with a somewhat larger-diameter antiproton plasma, which, however, lies well within the range of experimental parameters currently being used.

Beyond this expected increase in usable ultra-cold (sub-K) $\bar{H}$, two further modifications tied to the ELENA upgrade of the AD will positively impact the physics possibilities. On the one hand, an increase in experimental space allows the introduction of a broader range of spectroscopic tools and techniques. On the other hand, continuous operation of up to four experiments in parallel not only requires a greater degree of automation of the experiments, but also ensures a higher efficiency in developmental phases.

8. Conclusion

With the recent advances achieved in manipulating antiprotons and in forming and laser-exciting positronium, as well as the progress made towards (indirect) laser cooling of antiprotons, the significant increase in the number of trappable antiprotons made possible by the ELENA upgrade to the AD opens the door to the production of very large numbers of sub-K antihydrogen atoms. A concomitant effort is being made to also increase the number of useful Ps^*, so that these do not end up being a limiting factor.

With such expected large numbers of ultra-cold antihydrogen atoms, beam-based measurements of the gravitational deflection or of HFS of ground-state antihydrogen atoms in a field-free environment should play an important role in setting precision limits to violations of the weak equivalence principle or of CPT.

Authors' contributions. All authors contributed significantly to the design, implementation and operation of the experimental apparatus, to data taking and to the physics analysis, and provided critical feedback.

Data accessibility. This article has no additional data.

Competing interests. The authors declare that they have no competing interests.

Funding. This work was supported by: Istituto Nazionale di Fisica Nucleare; the Swiss National Science Foundation Ambizione grant (no. 154833); a Deutsche Forschungsgemeinschaft research grant; an excellence initiative of Heidelberg University; Marie Sklodowska-Curie Innovative Training Network Fellowship of the European Commissions Horizon 2020 Programme (no. 721559 AVA); European Research Council under the European Union's Seventh Framework Program FP7/2007–2013 (grant nos 291242 and 277762); Austrian Ministry for Science, Research and Economy; Research Council of Norway; Bergen Research Foundation; John Templeton Foundation; Ministry of Education and Science of the Russian Federation and Russian Academy of Sciences; and the European Social Fund within the framework of realizing the project, in support of intersectoral mobility and quality enhancement of research teams at Czech Technical University in Prague (grant no. CZ.1.07/2.3.00/30.0034).

References

1. Testera G *et al.* (AEgIS Collaboration). 2015 (The AEgIS experiment). *Hyperfine Interact.* **233**, 13–20. (doi:10.1007/s10751-015-1165-5)
2. Aghion S *et al.* (AEgIS Collaboration). 2014 A Moiré deflectometer for antimatter. *Nat. Commun.* **5**, 4538. (doi:10.1038/ncomms5538)
3. Hinterberger A, Gerber S, Doser M. 2017 Superconducting shielding with Pb and Nb tubes for momentum sensitive measurements of neutral antimatter. *J. Instrum.* **12**, T09002. (doi:10.1088/1748-0221/12/09/T09002)
4. Humbertson J, Charlton M, Jacobson F, Deutch B. 1987 On antihydrogen formation in collisions of antiprotons with positronium. *J. Phys. B: At. Mol. Phys.* **20**, L25–L29. (doi:10.1088/0022-3700/20/1/005)
5. Charlton M. 1990 Antihydrogen production in collisions of antiprotons with excited states of positronium. *Phys. Lett. A* **143**, 143–146. (doi:10.1016/0375-9601(90)90665-B)
6. Hessels EA, Homan DM, Cavagnero MJ. 1998 Two-stage Rydberg charge exchange: an efficient method for production of antihydrogen. *Phys. Rev. A* **57**, 1668. (doi:10.1103/PhysRevA.57.1668)
7. Storry C *et al.* (ATRAP Collaboration). 2004 First laser-controlled antihydrogen production. *Phys. Rev. Lett.* **93**, 263401. (doi:10.1103/PhysRevLett.93.263401)
8. Hogan S. 2016 Rydberg–Stark deceleration of atoms and molecules. *EPJ Techniq. Instrum.* **3**, 1. (doi:10.1140/epjti/s40485-016-0029-y)
9. Cassidy DB, Hisakado TH, Tom HWK, Mills Jr AP. 2012 Efficient production of Rydberg positronium. *Phys. Rev. Lett.* **108**, 043401. (doi:10.1103/PhysRevLett.108.043401)
10. Aghion S *et al.* (AEgIS Collaboration). 2016 Laser excitation of the $n = 3$ level of positronium for antihydrogen production. *Phys. Rev. A* **94**, 012507. (doi:10.1103/PhysRevA.94.012507)
11. Cassidy DB, Deng SHM, Tanaka HKM, Mills AP. 2006 Single shot positron annihilation lifetime spectroscopy. *Appl. Phys. Lett.* **88**, 194105. (doi:10.1063/1.2203336)
12. Aghion S *et al.* (AEgIS Collaboration). Submitted to EPJ.
13. Andresen GB *et al.* (ALPHA Collaboration). 2008 Compression of antiproton clouds for antihydrogen trapping. *Phys. Rev. Lett.* **100**, 203401. (doi:10.1103/PhysRevLett.100.203401)
14. Andresen GB *et al.* (ALPHA Collaboration). 2010 Evaporative cooling of antiprotons to cryogenic temperatures. *Phys. Rev. Lett.* **105**, 013003. (doi:10.1103/PhysRevLett.105.013003)
15. Krasnický D, Caravita R, Canali C, Testera G. 2016 Cross section for Rydberg antihydrogen production via charge exchange between Rydberg positroniums and antiprotons in a magnetic field. *Phys. Rev. A* **94**, 022714. (doi:10.1103/PhysRevA.94.022714)

16. Charlton M. 1997 Possible antihydrogen formation in antiproton–positronium reactions: where we've been and where we're going. *Hyperfine Interact.* **109**, 269–278. (doi:10.1023/A:1012669820504)
17. Andersen SL, Cassidy DB, Chevallier J, Cooper BS, Deller A, Wall TE, Uggerhøj UI. 2015 Positronium emission and cooling in reflection and transmission from thin meso-structured silica films. *J. Phys. B: At. Mol. Opt. Phys.* **48**, 204003. (doi:10.1088/0953-4075/48/20/204003)
18. Aghion S *et al.* (AEgIS Collaboration). 2017 Characterization of a transmission positron/positronium converter for antihydrogen production. *Nucl. Instrum. Methods Phys. Res. B* **407**, 55–66. (doi:10.1016/j.nimb.2017.05.059)
19. Kellerbauer A, Walz J. 2006 A novel cooling scheme for antiprotons. *New J. Phys.* **8**, 45. (doi:10.1088/1367-2630/8/3/045)
20. Pan L, Beck DR. 2010 Candidates for laser cooling of atomic anions: La^- versus Os^-. *Phys. Rev. A* **82**, 014501. (doi:10.1103/PhysRevA.82.014501)
21. Fesel J, Gerber S, Doser M, Comparat D. 2017 Optical dipole-force cooling of anions in a Penning trap. *Phys. Rev. A* **96**, 031401. (doi:10.1103/PhysRevA.96.031401)
22. O'Malley S, Beck D. 2010 Lifetimes and branching ratios of excited states in La^-, Os^-, Lu^-, Lr^-, and Pr^-. *Phys. Rev. A* **81**, 032503. (doi:10.1103/PhysRevA.81.032503)
23. Jordan E, Cerchiari G, Fritzsche S, Kellerbauer A. 2015 High-resolution spectroscopy on the laser-cooling candidate La^-. *Phys. Rev. Lett.* **115**, 113001. (doi:10.1103/PhysRevLett.115.113001)
24. Yzombard P, Hamamda M, Gerber S, Doser M, Comparat D. 2015 Laser cooling of molecular anions. *Phys. Rev. Lett.* **114**, 213001. (doi:10.1103/PhysRevLett.114.213001)
25. Tulej M, Knopp G, Gerber T, Radi PP. 2010 Degenerate and two-color resonant four-wave mixing of C_2^- in a molecular beam environment. *J. Raman Spectrosc.* **41**, 853–858. (doi:10.1002/jrs.2638)